ASTRONOMY & ASTROPHYSICS
SUPPLEMENT SERIES

Astron. Astrophys. Suppl. Ser. **122,** 43-49 (1997)

Monitoring MWC 560 ≡ V 694 Monocerotis in 1990-1995

II. Plate spectra⋆

T. Tomov and D. Kolev

National Astronomical Observatory Rozhen, P.O. Box 136, 4700 Smolyan, Bulgaria
e-mail: rozhen@tempus.tu-plovdiv.bg

Received January 4; accepted June 26, 1996

Abstract. We present the results of the photographic spectral observations of MWC 560 carried out in the period 1990–1993. The evolution of the spectrum, the changes in the radial velocities of the different line systems, as well as the variations in the equivalent widths of the different Balmer absorption components, are given and briefly discussed. The suggestion that the hot component of MWC 560 ejects high-velocity, highly-collimated jets along the line of sight, is in very good agreement with the observations. All the results, including the variations in the shapes, velocities and equivalent widths of the strong-shifted Balmer absorptions, confirm that compact companion in MWC 560 ejects matter in two different regimes – *discrete* and *quasi-stationary*. It is supposed that the permanent presence of a relatively weak and small-shifted Balmer absorption component in the spectrum, indicates additional persistent, not spherically symmetric matter outflow.

Key words: accretion, accretion disks — stars: activity — stars: binaries: symbiotic — stars: individual: MWC 560 — stars: mass–loss

1. Introduction

MWC 560 is a peculiar system which became popular in the beginning of 1990 when it was caught in the strongest outburst ever recorded (Tomov 1990; Tomov et al. 1990). Now it is accepted that MWC 560 is a symbiotic-like system consisting of an M4–5III cool component (Thakar & Wing 1992) and a white dwarf probably possessing a strong magnetic field (Tomov et al. 1992, 1994; Michalitsianos et al. 1993). The interaction of the matter accreted from the giant's stellar wind with the rapidly rotating magnetosphere, as well as high-velocity matter ejection along the line of sight, can account for many of the observed features in the brightness and the spectrum (Tomov et al. 1992, 1994; Shore et al. 1994; Tomov et al. 1996, hereafter Paper I).

The star brightness shows a large variety of long and short-term changes. In Paper I we presented the UBV photometric behaviour of MWC 560 during 1990–1995.

Because of the unique character of the spectrum of MWC 560, it is important to show its evolution in detail. In this paper we present results from our vast collection of photographic spectra in the optical region, obtained in the period 1990–1993. In Paper III we shall report on high and low resolution CCD observations of MWC 560 we have obtained since 1990 at a number of different observatories.

2. Observations

The spectra were obtained in the coudé-spectrograph of the 2-m telescope at Rozhen Observatory (Bulgaria) with typical exposure times of 2–3 hours. Hydrogen treated, 103aO emulsion was used. Each plate covered a spectral interval from 3600 Å to 4950 Å and had a spectral resolution of about 0.35 Å. Iron-argon hollow cathode lamp spectrum was obtained for wavelength calibration and the photometric calibration was achieved by 10–steps sensitometer exposures on each plate. The typical S/N ratio on the local continuum level was 10–15.

The spectra were digitized by MDM6 Joyce Loebl microdensitometer, with 20 μ wide slit and 10 μ step. We used the software system ReWiA (Borkowski 1988) to process the data. The spectra were linearized using dispersion curves of not less than ± 0.05 Å accuracy.

All the spectra shown in Figs. 1, 2 and 3 are normalized to the local continuum level and shifted for plot clarity.

In Tables 1 and 3 and Figs. 4 and 5 single measurements of equivalent widths and peak intensities of some spectral features are presented. The accuracy of these measurements depends on two reasons mainly: i) the typical errors associated with the photographic emulsion

Send offprint requests to: T. Tomov

⋆ Tables 1, 2, 3 only available in electronic form at CDS.

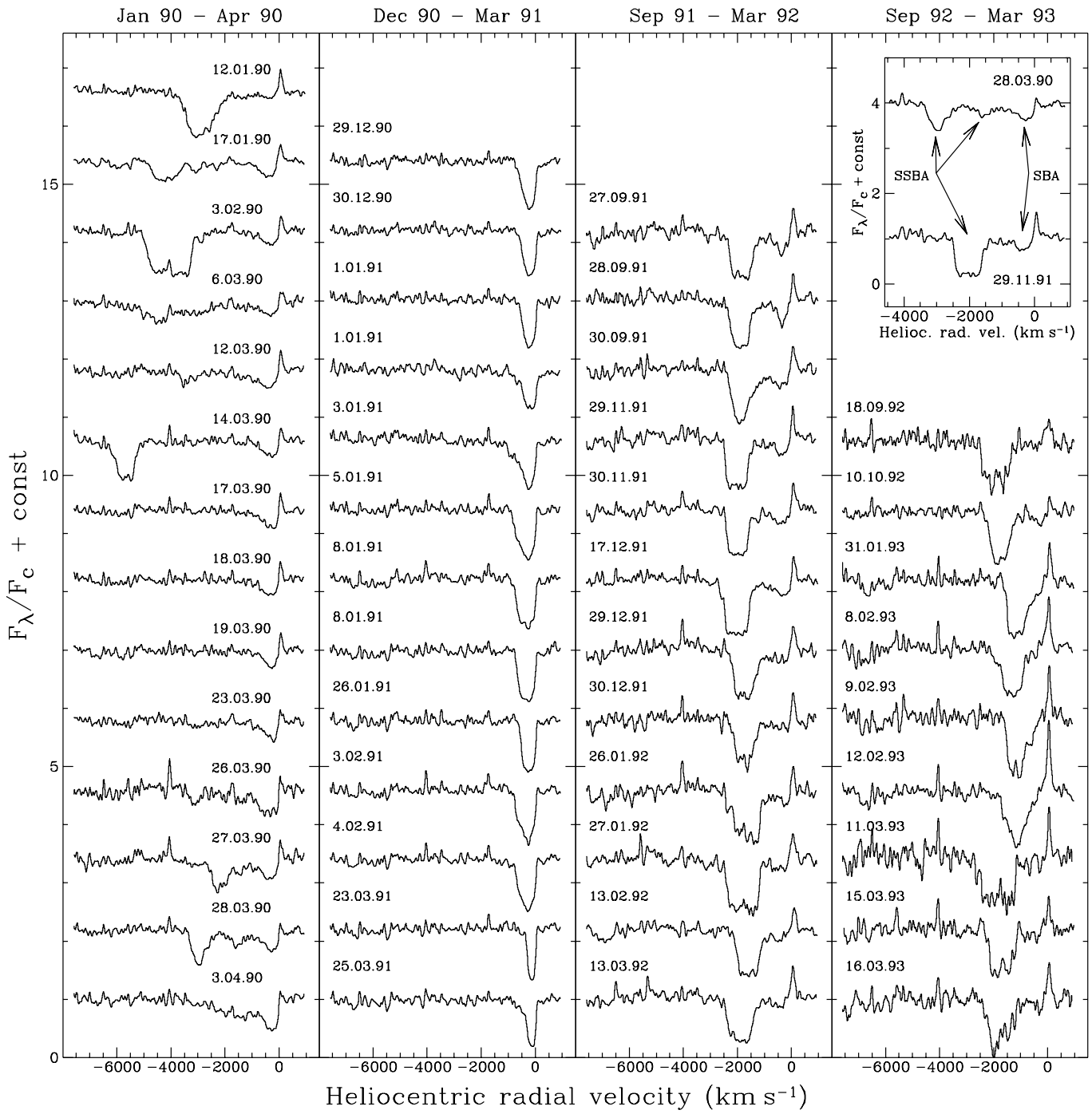

Fig. 1. The evolution of $H\delta$ over the whole period of observation. Each observing season is shown in a separate panel. In the upper part of the rightmost panel an additional picture is inserted to define the different types of Balmer absorption components – SSBA (strong shifted Balmer absorptions) and SBA (slowest Balmer absorptions)

which can be up to $\pm 10 - 15\%$ and ii) the difficulties arisen during the continuum level fitting procedure. We can assume a value of about 20% as an upper limit for the errors in these single measurements.

3. Results

3.1. General description and changes of the MWC 560 spectrum

The energy distribution in the optical may be best understood as a combination of an M4.5III + B5–A0 star.

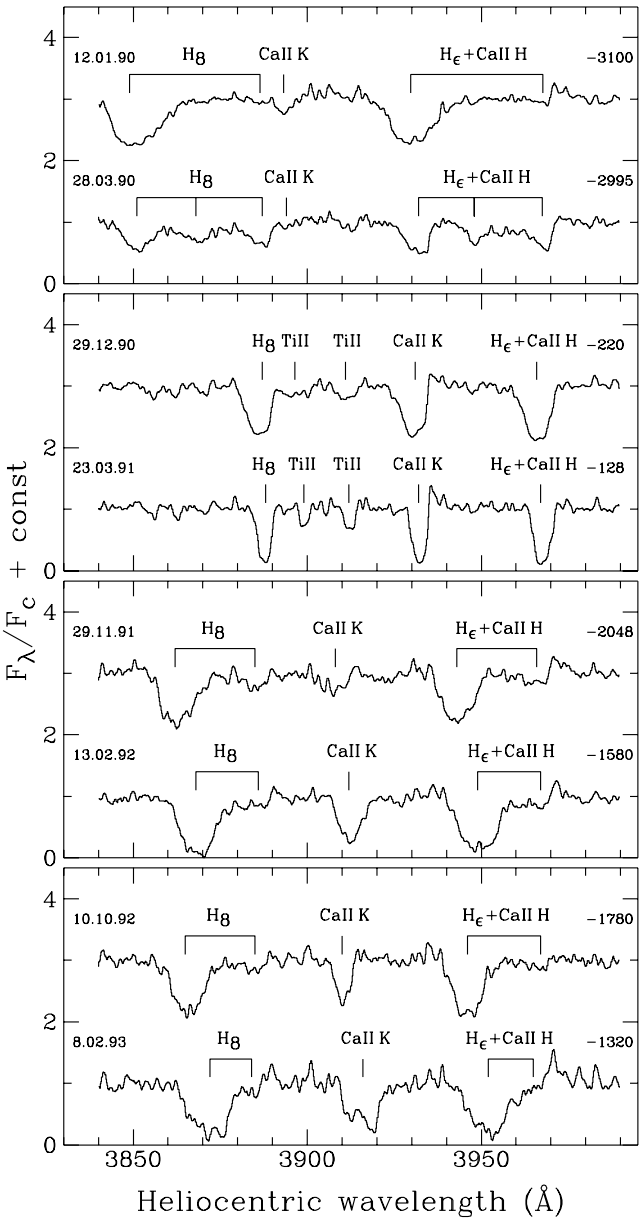

Fig. 2. The spectral region around H_8, CaII K and H_ε in the spectrum of MWC 560. Each observing season is represented by two spectra. The horizontal and vertical marks show the different absorption lines and their components. The negative numbers on the right side represent the radial velocity of the absorptions with the highest shifts in each spectrum

Zhekov et al. (1996) have shown that the "luminosity class" of the hot source in this binary changes. During the state of high ejection activity (January–April 1990, see below) it resembled a *supergiant* while since late 1990 it is more like a *main sequence* star.

The line spectrum of MWC 560 can be also considered as a combination of two different components: i) absorption line systems with different radial velocity (RV), and ii) emission spectrum with almost constant look (Kolev & Tomov 1993). The behaviour of both types of spectra is quite different.

The Balmer lines dominate the absorption spectrum of MWC 560. A complete view of the MWC 560 spectrum is published earlier (Kolev & Tomov 1993). In Fig. 1 we present the evolution of H_δ using all the plate spectra obtained in the period 1990–1993. H_δ was chosen because it is relatively free of strong blending. The panels of the figure are arranged according to the annual observing seasons of MWC 560 but in fact this arrangement follows also the different behaviour of the absorption spectrum.

The distinctions between the absorption components of H_δ in the different observing seasons are clearly visible in Fig. 1. The intensity and radial velocity variations of these components during the seasons after April 1990 are less appreciable in comparison with the changes during January–April 1990. The observed behaviour of the strong shifted Balmer absorption components in the whole period 1990–1993 is in a good agreement with the supposed *discrete* and *quasi-stationary* regimes of matter ejection (Tomov et al. 1992; Kolev & Tomov 1993).

The spectral observations of MWC 560 since 1990 give us reasons to assume that in addition to the high-velocity matter ejection a continuous low-velocity mass-loss takes place as well. On all spectra, with the exception of these obtained in 1990/1991, a weaker, relatively wide absorption component with a velocity of about -280 km s^{-1} is present in all Balmer lines (Figs. 1–3).

The Balmer absorption components show a very complicated picture and for the sake of clarity the nomenclature of the various absorptions is given in an additional figure inserted in the rightmost panel in Fig. 1. The *strong shifted Balmer absorptions* (SSBA) are connected with the *discrete* and *quasi-stationary* matter ejection, while the *slowest Balmer absorptions* (SBA) indicate the continuous low-velocity mass-loss.

Other absorption lines that are permanently present or appear in different moments in the spectrum of MWC 560 are the components of CaII K, HeI and some ions and neutral metals (mainly Fe and Ti). Figures 2 and 3 show the behaviour of these lines on two typical spectra obtained in each season. The components of CaII K have the same RVs and shapes as those of Balmer lines. The K-line was weakest during January–April 1990 and in the first half of the 1991/1992 season. During the rest of the time these absorptions were very strong, often comparable with the Balmer ones (Fig. 2). There are two HeI lines – 4471 Å and 4026 Å, confidently present in most of the spectra of MWC 560. The absorption components of these lines are usually very weak. Their violet-shifts are of the same order as these of the hydrogen and CaII absorptions. In Fig. 3 the position of the weak HeI 4471 Å absorption is indicated by an arrow in the spectra in which this component is present.

A noticeable absorption of MgII 4481 Å appeared in the spectrum of MWC 560 in 1990/1991 only (thick

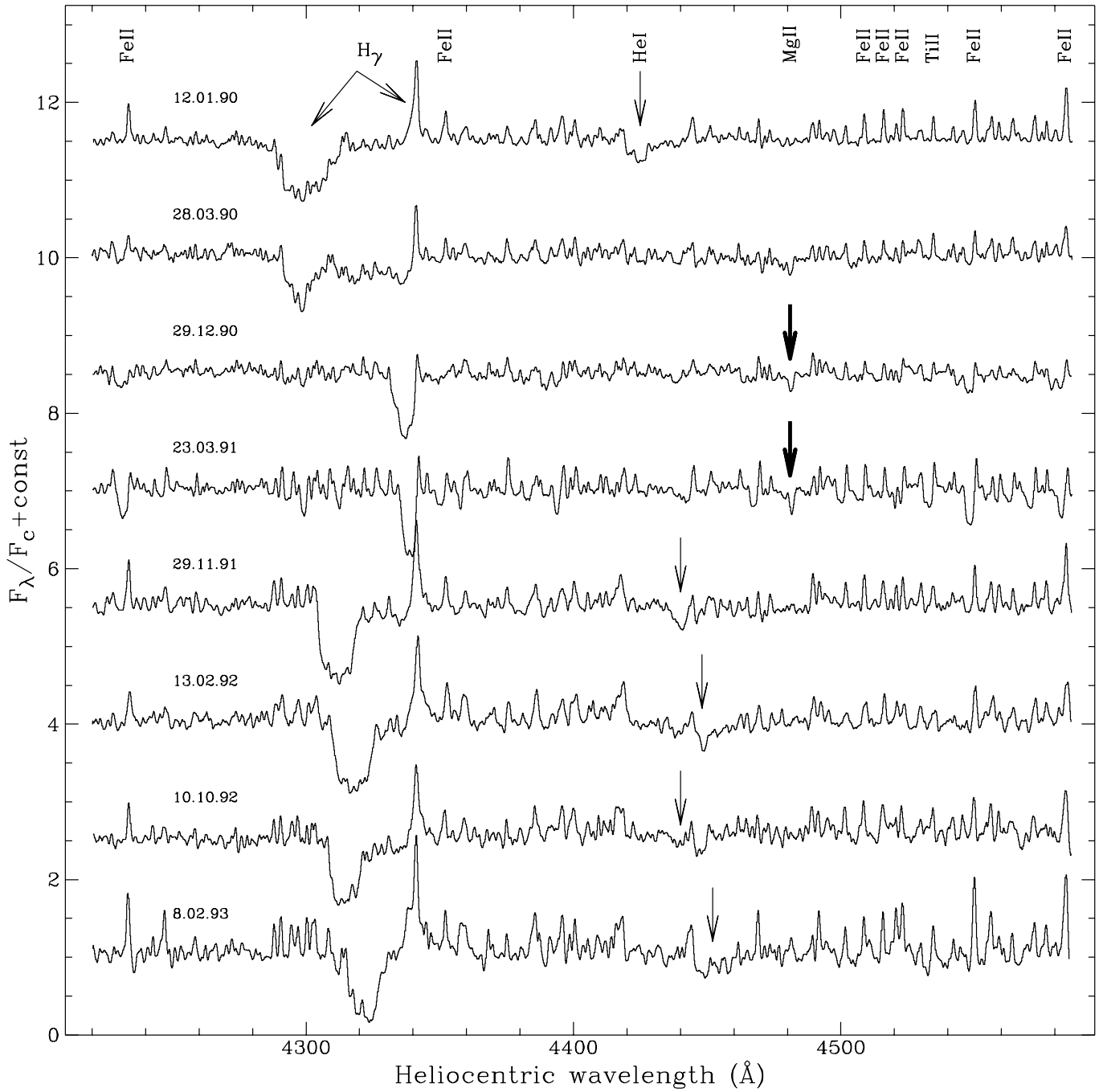

Fig. 3. The spectral region around H_γ in the spectrum of MWC 560. Each observing season is represented by the same two spectra used in Fig. 2. The weak HeI absorptions are marked by *thin arrows* and the MgII absorption is marked by *thick arrows*

arrows in Fig. 3). This absorption shows considerably small violet-shift. We measured an average radial velocity -0.9 ± 2.8 km s^{-1} for this line.

The emission spectrum of MWC 560 is dominated by the lines of the singly ionized metals, mainly FeII and TiII (cf. Kolev & Tomov 1993). The singly ionized metals show strong absorption components during the observing season 1990/1991 only (Figs. 2, 3). These components are equally violet-shifted as the SSBA. The strongest one is a TiII absorption blend at 3760 Å which exceeds in intensity the nearest Balmer lines H11 and H12. This TiII blend is the only absorption (in addition to the hydrogen, CaII and HeI ones) which is intensive enough in the spectra obtained in 1992/1993.

Figure 3 shows an example of the emission spectrum of MWC 560. The same lines are present in the MWC 560 spectrum all the time being very sharp and positional stable. We chose the emission lines FeII 4515 Å

and TiII 4590 Å, which do not show remarkable absorption components, to make a rough estimate of their variations. The equivalent width W_λ and the peak intensity I_λ in continuum units are plotted in Fig. 4. One can note a small decrease of W_λ (FeII) in 1990/1991 which may be explained by influence of a weak absorption component. It is possible also to note a small gradual increase of W_λ and I_λ for both lines but the large data scatter prevents more definite conclusions.

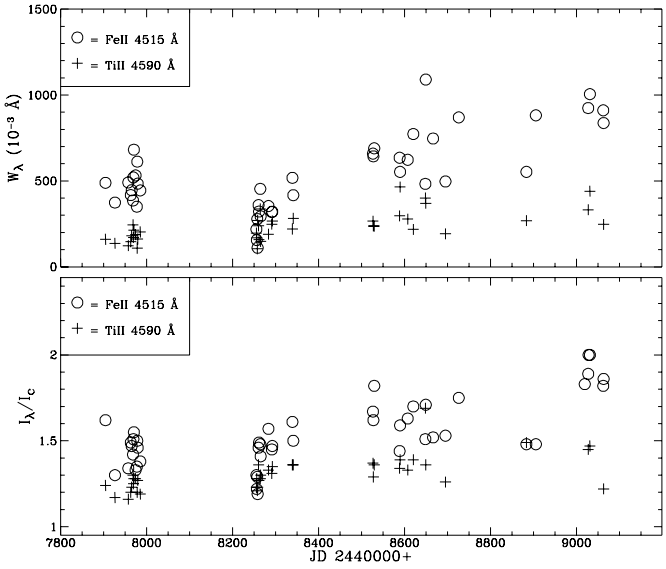

Fig. 4. Equivalent widths (*Top*) and peak intensities (*Bottom*) of the FeII 4515 Å and TiII 4590 Å emission lines

3.2. Line formation regions

Comparing the profile shapes and the behaviour of the Balmer lines in the period under discussion, it is obvious that they are far from the classical P Cyg-type (Figs. 1–3). Their stationary emission components are much narrower and completely detached from the absorption ones. The observed conspicuous variations of the SSBA do not reflect in any way on the emission components. In particular, during the *discrete* ejections, it is clearly visible that the appearance and disappearance of the SSBA as well as the variations in their intensities, shapes and velocities are not connected with changes in the position, shape and intensity of the emission components (Fig. 1). This indicates that the emission and strong absorption components of the Balmer lines in the spectrum of MWC 560 originate in different regions with different physical conditions.

The simplest way to explain the strong shifted absorptions is a highly collimated jet which has a significant covering factor to obscure the central source (Tomov et al. 1990, 1992; Shore et al. 1994). An important question is where the emission lines originate – around the hot component or in the M giant atmosphere? We suggested that the emission lines originate in the outer parts of an accretion disk, supposing a *face-on* geometry for the MWC 560 system. The same was argued recently by Shore et al. (1994).

Near infrared photometry shows that the cool component behaves like a normal M4-5 giant (cf. Buckley 1992; Zhekov et al. 1996). On the other hand, if the emissions are formed in the M giant atmosphere they must be superimposed on the composite spectrum. It is evident in Fig. 3 that when the metal emissions are blended with the strong H_γ absorption they are weakened. The emission components of H_δ (Fig. 1) and H_γ (Fig. 3) in 1990/1991 are affected in the same way by the red wings of their absorptions. This shows that the outflowing gas in which the SSBA originate is projected on the emission lines formation region and can absorb a part of its radiation. Therefore, the emissions most probably arise around the hot component and not in the M giant's atmosphere.

The hydrogen and ionized metals profiles in 1990/1991 closely resemble the P Cyg-type only because of the smaller ejection velocities.

We examined the changes in the intensities and velocities of the SBA component in the period 1990–1993 with the exception of 1990/1991 observing season. Its equivalent widths (W_λ) and radial velocities are listed in Table 1 and examples of the variations of the W_λ and RV are given in Fig. 5. The changes in the W_λ of this absorption are not great during each season as well as during all the time since 1990. The first members of the Balmer series ($H_\beta - H_\varepsilon$) show more negative RV in comparison to the higher members (Fig. 5). This difference is probably caused by the blending with the Balmer emissions. The lines after H_ε do not show emission components and the SBA velocities are practically constant.

On our photographic spectra we did not find, even in H_β, H_γ (Fig. 3) and H_δ (Fig. 1), emission wings as wide as the SBA. We suppose that the SBA components which are permanently present in the spectrum of MWC 560 arise in a persistent mass-outflow with a velocity of about 280 km s^{-1}. The lack of real P Cyg profiles probably indicates that this outflow is not spherically symmetric.

3.3. Radial velocities

Table 2 presents the average heliocentric RV of the main absorption and emission features. Some of the spectra were measured independently more than once.

The Balmer emission components show more positive and largely scattered RV in comparison to the metallic ones (Table 2). This difference is not caused by a physical reason but it is a result of an influence of the red wing of the SBA component.

The RVs of the metallic emission lines are plotted in Fig. 6, where the enlarged symbols signify the spectra being measured more than once. No systematic changes can be noted during the four years' monitoring of MWC 560. The scattering of the points around the mean radial

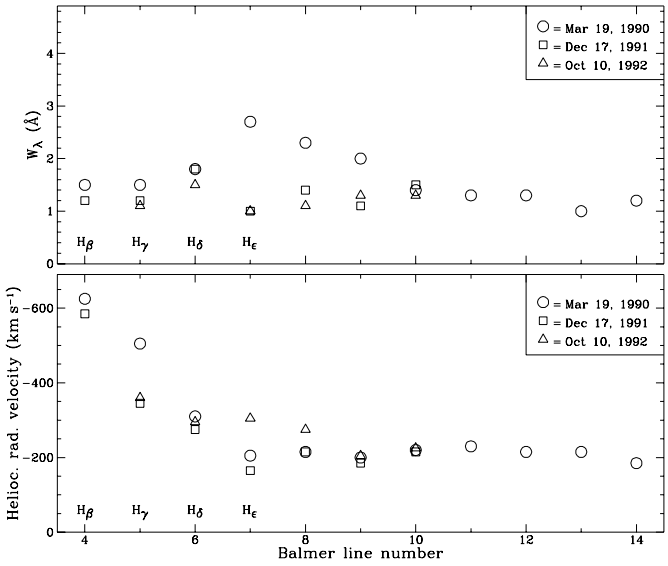

Fig. 5. Examples of the radial velocities (*Bottom*) and W_λ (*Top*) of the SBA components in the spectrum of MWC 560

velocity +35.5 km s^{-1} (Fig. 6) is rather of the order of the measurement errors. The periodogram analysis of the data, performed using the Lafler & Kinman (1965); Deeming (1975); Stellingwerf (1978) and Schwarzenberg–Czerny (1989) methods, does not show any significant period in the range of 100 − 2000 days.

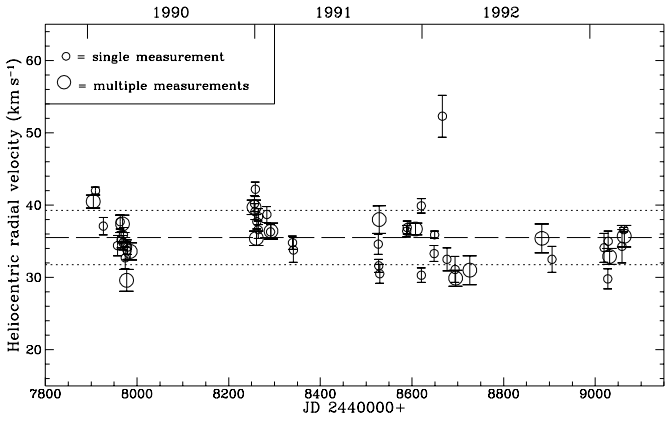

Fig. 6. Radial velocities of the metallic emission lines in the spectrum of MWC 560. The *long dashed line* and the *short dashed lines* mark the mean velocity of +35.5 km s^{-1} and the 3σ limits respectively

Chentsov (1994, private communication) has made high-accuracy RV measurements of the emission and absorption lines on two CCD spectra in the near infrared region obtained in 1992 and 1993. These measurements include the emission lines of the same single ionized metals, as the ones observed in the optical region and the absorption lines of the neutral metals surely belonging to the M giant spectrum. They show practically identical RVs with a mean value of +35.8 km s^{-1}.

The lack of noticeable variations in the RVs of the single ionized metals emissions and the coincidence of these velocities with those of the M giant absorptions do not contradict to a *face-on* location of the MWC 560 system orbital plane.

The SSBA radial velocities, as well as these of CaII K show a picture (Fig. 7) in very good agreement with the two regimes of matter ejection. During the *discrete* ejections period (January–April 1990) the strong shifted absorption RVs change with amplitude more than 4000 km s^{-1}. These velocities cover an interval from −1000 km s^{-1} to about −6000 km s^{-1} around the star brightness maximum (cf. Paper I) – the highest value ever observed. The RVs of the SSBA change in very short timescales. Even on spectra obtained in two-three days interval, if the SSBA are present, their violet shifts may differ by several thousands of km s^{-1} (Figs. 1 and 7, Table 2).

In the next observing seasons, when the matter ejection is *quasi-stationary*, the RVs of SSBA show completely different behaviour. The changes within each season are much smaller in comparison to January–April 1990. The RVs observed in 1990/1991 remarkably differ from all the rest and are from −130 to −320 km s^{-1}. While, during the next two observing seasons (1991/1992 and 1992/1993) the radial velocities range from −1200 to −2000 km s^{-1} (Fig. 7, Table 2).

As it was shown earlier (Tomov et al. 1994), the integrated ultraviolet flux changes in the same way as the RVs of the SSBA during the different observing seasons.

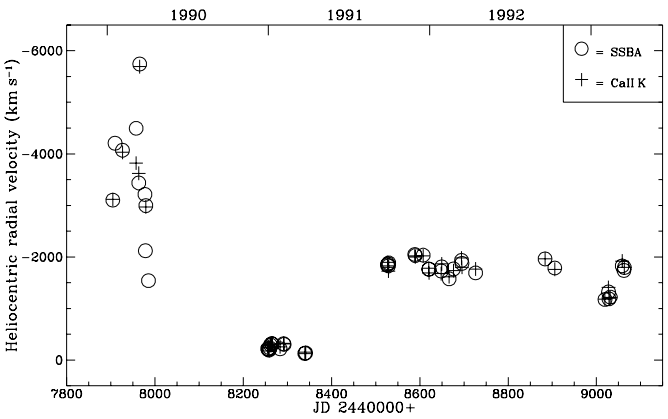

Fig. 7. Radial velocities of the SSBA components and CaII K strong–shifted absorptions in the spectrum of MWC 560. The measurement errors are not shown here because they are very small in comparison to the RV values (cf. Table 2)

3.4. SSBA equivalent widths

The equivalent widths W_λ of the most intensive SSBA in all spectra are presented in Table 3. The average values for the time intervals distinguished by different regimes of matter ejection are plotted in Fig. 8 in respect to the Balmer line numbers.

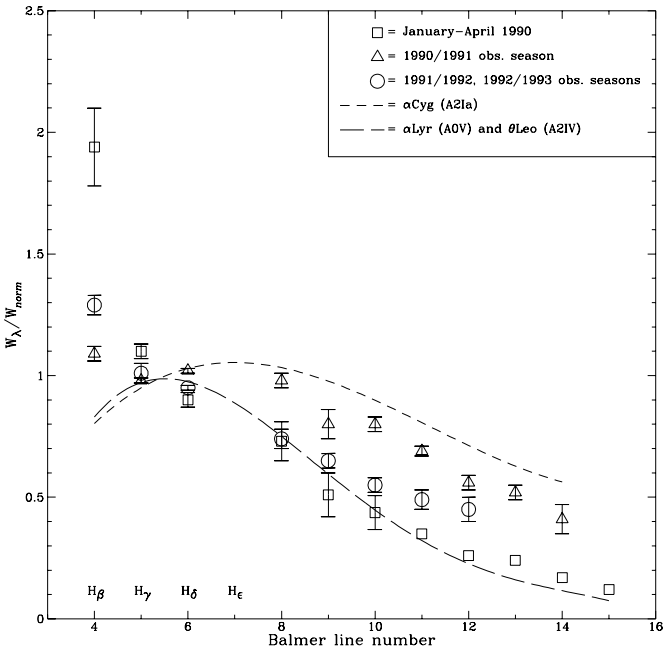

Fig. 8. The normalized average equivalent widths of the SSBA in the MWC 560' spectrum in different observing seasons in respect to the line numbers. The error bars for the lines after H10 in the period January–April 1990 are not shown because the measurements are made on the basis of a single spectrum.The data for the normal supergiant αCyg are taken from Leedjärv & Iliev (1989)

We chose the half-sum of the W_λ of H_γ and H_δ in each plate as an internal normalization unit

$$W_{\rm norm} = [W_\lambda(H_\gamma) + W_\lambda(H_\delta)]/2 \qquad (1)$$

because both lines are best measurable in all spectra.

The relation, in the case of *discrete* high-velocity ejections, is the steepest one and after $n = 6$ entirely coincides with the relation for normal main sequence A0–A2 star. The relation for the 1990/1991 observing season, when a *quasi-stationary* ejection with low velocities was observed, resembles rather those for a supergiant of the same spectral type. The case of *quasi-stationary* ejection with high velocities, during 1991/1992 and 1992/1993 observing seasons, shows an intermediate picture. The resemblance of the relations for MWC 560 in different moments with the main sequence or the supergiant stellar ones probably indicates the changes in the optical depth, the density and the velocities of the media where the absorptions arise.

Acknowledgements. We thank E.L. Chentsov who kindly provided us with unpublished radial velocities in the near infrared region. We also thank Ulisse Munari for the very constructive comments. This research has been sponsored by the Bulgarian National Foundation for Scientific Research under contract F-35/1991. We are grateful to the anonymous referee for critical comments.

References

Borkowski J., 1988, ReWiA – Instrukcja obsługy, Torun Observatory, Poland (in Polish)
Buckley D.A.H., 1992, Kondo Y. et al. (eds.), Evolutionary Processes in Interacting Binary Stars, p. 421
Deeming T.J., 1975, Ap&SS 36, 137
Kolev D., Tomov T., 1993, A&AS 100, 1
Lafler J., Kinman T.D., 1965, ApJS 11, 216
Leedjärv L., Iliev I., 1989, The Spectrum of Deneb. An Atlas λλ3668–5014 Å., Valgus, Tallin
Michalitsianos A.G., Perez M., Shore S.N., et al., 1993, ApJ 409, L53
Schwarzenberg–Czerny A., 1989, MNRAS 241, 153
Shore S.N., Aufdenberg J.P., Michalitsianos A.G., 1994, AJ 108, 671
Stellingwerf R.F., 1978, ApJ 224, 953
Thakar A., Wing R.F., 1992, BAAS 24, 801
Tomov T., 1990, IAU Circ. 4955
Tomov T., Ivanov M., Antov A., 1996, A&AS 116, 1 (Paper I)
Tomov T., Kolev D., Georgiev L., et al., 1990, Nat 346, 637
Tomov T., Kolev D., Michalitsianos A.G., et al., 1994, MemSAIt 65, 167
Tomov T., Zamanov R., Kolev D., et al., 1992, MNRAS 258, 23
Zhekov S.A., Hunt L.H., Tomov T., Gennari S., 1996, A&A 309, 800